PROCEEDINGS OF SPIE

SPIEDigitalLibrary.org/conference-proceedings-of-spie

ZnO nanostructures for organometallic halide perovskite solar cells

Ho Won Tam, Fangzhou Liu, Yushu Wang, Wei Chen, Tik Lun Leung, et al.

Ho Won Tam, Fangzhou Liu, Yushu Wang, Wei Chen, Tik Lun Leung, Aleksandra B. Djurišić, Alan Man Ching Ng, Wai Kin Chan, Jinyao Tang, "ZnO nanostructures for organometallic halide perovskite solar cells," Proc. SPIE 10533, Oxide-based Materials and Devices IX, 105332Q (23 February 2018); doi: 10.1117/12.2291595

SPIE.

Event: SPIE OPTO, 2018, San Francisco, California, United States

ZnO nanostructures for organometallic halide perovskite solar cells

Ho Won Tam[a], Fangzhou Liu[a], Yushu Wang[a], Wei Chen[a,b], Tik Lun Leung[a], Aleksandra B. Djurišić*[a], Alan Man Ching Ng[c], Wai Kin Chan[d], Jinyao Tang[d]
[a]Department of Physics, The University of Hong Kong, Hong Kong, China;
[b]Department of Materials Science & Engineering, South University of Science and Technology of China, Shenzhen, China;
[c]Department of Physics, South University of Science and Technology of China, Shenzhen, China;
[d] Department of Chemistry, The University of Hong Kong, Hong Kong, China

ABSTRACT

ZnO is considered a potential alternative of TiO_2 for electron transport materials of perovskite solar cells due to its relatively high electron mobility and the ease of low temperature solution-processing. Nevertheless, ZnO-based perovskite devices usually exhibit inferior device performance and stability compared to TiO_2 based devices due to the defect states at ZnO/perovskite interface. In this study, an ultrathin TiO_2 layer by ALD is applied to ZnO nanostructures, and its effect on device performance is investigated. The results indicate that TiO_2 ultrathin layer can effectively passivate the surface of ZnO nanostructures, resulting in enhanced device performance.

Keywords: perovskite, zinc oxide, solar cells, atomic layer deposition

1. INTRODUCTION

Organometallic halide perovskite solar cells (PSCs) have drawn great attention as the next generation solar cells in the recent years. Significant progress has been achieved in improving the power conversion efficiency (PCE) of perovskite solar cells since the first reports of solid-state perovskite solar cell devices in 2012[1-3], with the record efficiency increased from ~10%[2, 3] to over 22%.[4] TiO_2 is the most common material for inorganic electron transport layer (ETL) among various reported device architectures, with both the planar form and mesoporous form of TiO_2 ETL extensively studied in the literature. On the other hand, ZnO is regarded as a potential alternative electron transport material to conventional TiO_2 due to its wide band gap and relatively high electron mobility which promotes faster electron transport.[5-12] ZnO has a rich family of nanostructures which can be readily synthesized by solution process at low temperatures which is favorable for fabrication of flexible devices. The electrical and optical properties of ZnO nanostructures are largely dependent on their morphologies and can be easily tuned by doping or manipulating the composition. Till now, both the use of ZnO compact layers[5] and ZnO nanorod (NR) arrays[6-12] as the ETL for perovskite solar cells have been demonstrated in several studies. In particular, one dimensional ZnO nanorods are considered of high potential due to their high aspect ratios which will enhance charge collection at ZnO/perovskite interface and thus short circuit current. Nevertheless, photovoltaic performance of perovskite solar cells with ZnO ETL is still inferior compared to TiO_2 based devices. The inferior performance can be attributed to nonoptimized ZnO nanostructure morphologies, as well as recombination losses due to surface defects of ZnO. In addition, defects at ZnO/perovskite interfaces can also lead to decomposition of perovskite absorbers resulting in instability of the devices.[13-15]

To enhance the photovoltaic performance of ZnO based PSCs, efforts have been made by engineering the ZnO/perovskite interface to passivate the defect states and reduce the unfavorable charge recombination.[8-12] For example, a thin dipole layer of ethanolamine or polyethyleneimine can efficiently suppress the surface defects of ZnO ETL resulting in enhanced power conversion efficiency.[9] Core-shell nanoarchitechtures based on ZnO nanostructures are also reported to improve the photovoltaic performance. Ultrathin layer of Al-doped ZnO (AZO)[10], Al_2O_3[11], as well as TiO_2 [12]have been employed as the surface coating of ZnO nanostructures, resulting in increased power conversion efficiency. In this work, we report an ultrathin surface coating of TiO_2 by atomic layer deposition (ALD) technique for ZnO

Oxide-based Materials and Devices IX, edited by David J. Rogers, David C. Look, Ferechteh H. Teherani, Proc. of SPIE Vol. 10533, 105332Q · © 2018 SPIE
CCC code: 0277-786X/18/$18 · doi: 10.1117/12.2291595

nanostructures as the electron transport layer of perovskite solar cells. The use of ALD for TiO_2 coating enables precise control of the thickness as well as high uniformity and reproducibility of the coating. Perovskite solar cells with both ZnO compact layers and nanorods as the ETL are prepared, and the photovoltaic performance of the devices with and without TiO_2 passivation layer is compared. Influence of the TiO_2 layer thickness on the device performance is also investigated. It is found that at optimized thickness, TiO_2 surface coating on ZnO nanostructures can effectively improve the photovoltaic performance of the perovskite solar cells.

.

2. EXPERIMENTAL DETAILS

2.1 Materials

Lead iodide (PbI_2, 99.9985%), N,N-Dimethylformamide (DMF, anhydrous, 99.9+%), and 2-propanol (anhydrous, 99.5+%) were obtained from Alfa Aesar. Zinc acetate (99.99%), zinc nitrate hydrate (99.999%), 2-methoxyethanol (≥99.3%), ethanolamine (≥99.0%), hexamethylenetetramine (≥99.0%), polyethyleneimine, bis (trifluoromethane) sulfonamide lithium salt (Li-TFSI, 99.95%), 4-tert butylpyridine (96%), chlorobenzene (≥99.5%), acetonitrile (anhydrous, 99.8%), and tetrakis(dimethylamino)titanium (TDMAT) were purchased from Sigma Aldrich. Methylammonium iodide (MAI) was purchased from Dyesol. 2,2',7,7'-Tetrakis[N,N-di(4-methoxyphenyl)amino]-9,9'-spirobifluorene (spiro-OMeTAD) was purchased from Shenzhen Feiming Co., Ltd.

2.2 Preparation of ZnO nanostructure

Patterned FTO/glass substrates were cleaned by sonication in acetone, toluene, acetone, ethanol, and deionized water in sequence, followed by UV ozone treatment for 300 s before use. ZnO nanorods were synthesized on FTO/glass substrates by hydrothermal growth method. In brief, a sol-gel precursor solution was prepared by dissolving 40 mg zinc acetate in 1 mL of 2-methoxyethanol with the addition of 3 wt% ethanolamine. The precursor solution was then heated at 80 °C under continuous stirring for 1 hour before use. ZnO seed layer was deposited onto FTO/glass substrates by spin coating the precursor solution at 3000 rpm for 30s, followed by preheating at 150 °C for 5 min and annealing at 350 °C for 1 hour. For hydrothermal growth of ZnO nanorods, the as prepared substrates with ZnO seed layer were placed upside down in a Petri dish and immersed in 75 mL aqueous solution containing 0.56 g zinc nitrate hydrate, 0.1 g polyethyleneimine, and 0.26 g hexamethylenetetramine at 90 °C. ZnO nanorods with different growth time were obtained for further characterization.

2.3 Atomic layer deposition of TiO_2 thin layer

TiO_2 thin layer was coated directly on the as prepared ZnO nanostructures using a Cambridge NanoTech Savannah 200 Atomic Layer Deposition System at different thicknesses. TDMAT was used as titanium precursor and H_2O was used as oxidizer. The deposition was conducted at 250 °C with a deposition rate of ~0.03 nm per cycle. 1 nm, 3 nm, 5 nm, and 10 nm of TiO_2 layers are deposited on ZnO nanostructures respectively.

2.4 Fabrication of perovskite solar cells

$CH_3NH_3PbI_3$ perovskite films were synthesized by a conventional 2-step method as reported previously.[16] PbI_2 was dissolved in DMF at a concentration of 1 M and stirred at 70 °C for 2 hours, while MAI was dissolved in isopropanol at 30 mg/mL at room temperature. PbI_2 solution was first spin coated on the substrates at 3000 rpm for 30 s, followed by drying at 70 °C on a hot plate for 20 min. MAI solution was then dropped onto PbI_2 layer and waited for 1 min before spin coating at 3000 rpm for 30 s. The perovskite films prepared on ZnO nanostructures with TiO_2 passivation layers were annealed at 100 for 5 min, while the perovskite films prepared on ZnO nanostructures without passivation layer were annealed at 70 °C for 30 min.

For hole transport layer (HTL), a precursor solutions as prepared by dissolving 72.3 mg of spiro-OMeTAD in 1 mL of chlorobenzene solution with 28.8 µL 4 tert-butylpyridine and 17.5µL Li-TFSI solution (520 mg Li-TFSI in 1 mL acetonitrile). The precursor solution was spin coated on perovskite film at 4000 rpm for 30 s and then annealed in an oxygen rich atmosphere at 40 °C in oxygen atmosphere for 2 hours. Finally, 15 nm of MoO_3 and 50 nm of Al were deposited as the contact electrodes via thermal evaporation.

2.5 Materials and device characterization

Morphological characterization of ZnO nanorods and perovskite films synthesized on different ZnO nanostructures was performed using a JEOL JMS-7001F scanning electron microscope (SEM). X-ray diffraction (XRD) patterns of as prepared ZnO nanostructures were measured on a Bruker D8 advance diffractometer using Cu Ka radiation (λ= 0.154184 nm) as radiation source. Photovoltaic performance of perovskite solar cells was evaluated by measuring the current-voltage (I-V) curves under simulated AM 1.5G illumination from ABET Sun 2000 solar simulator at a power density of 100 mW/cm^2. All devices were encapsulated inside the glovebox before characterization. The J-V curves were obtained by scanning in the range between 1.2 V and -0.2 V with a step of 0.1 V and a delay time of 0.1 s.

3. RESULTS AND DISCUSSION

Figure 1 shows the SEM images of ZnO thin films prepared by sol-gel method. Figure 2 shows the SEM images of ZnO nanorods with different growth time. It can be observed that the morphologies of the ZnO nanorods are largely affected by the growth time. Longer growth time results in increased rod diameter and length, and consequently increased aspect ratio. XRD patterns of the as grown ZnO nanorods and ZnO nanorods with 5 nm TiO_2 coating is shown in Figure 3. A sharp peak at 34.8 ° corresponding to ZnO (002) plane is observed in both samples. However, no peaks corresponding to TiO_2 are detected in ZnO nanorods with 5 nm TiO_2 layer, which may due to the ultrathin thickness of the TiO_2 layer, or the TiO_2 layer by ALD is in amorphous phase.

Figure 4 shows the SEM images of perovskite films prepared on different ZnO ETLs. Slight variations in the grain sized are observed for the perovskite films synthesized on as grown ZnO nanostructures and ZnO nanostructures with TiO_2 passivation layers. Moreover, with the addition of TiO_2 passivation layer, higher annealing temperature of perovskite films is allowed (100°C for ZnO/TiO_2 ETL and 70 °C for as prepared ZnO ETL). This indicates enhanced thermal stability of perovskite films due to efficient passivation of defect states at ZnO surface by TiO_2 ultrathin layer.

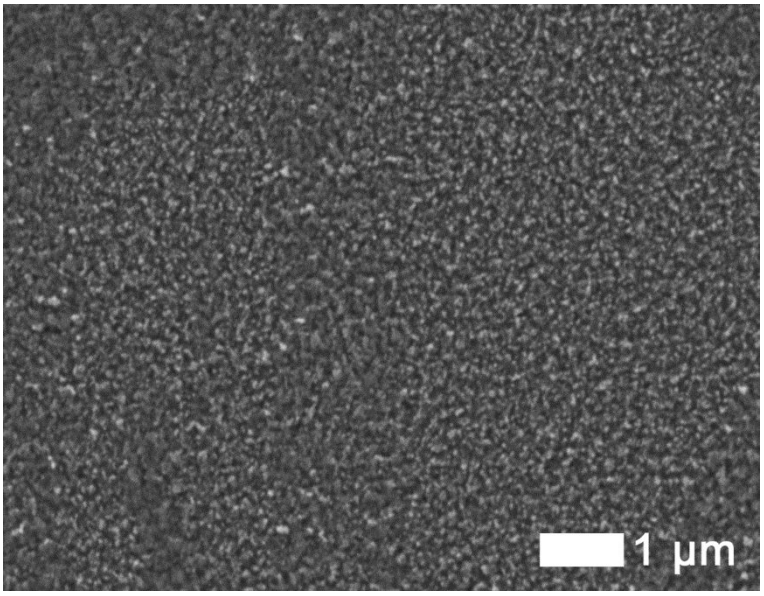

Figure 1. SEM image of ZnO thin film prepared by sol-gel method.

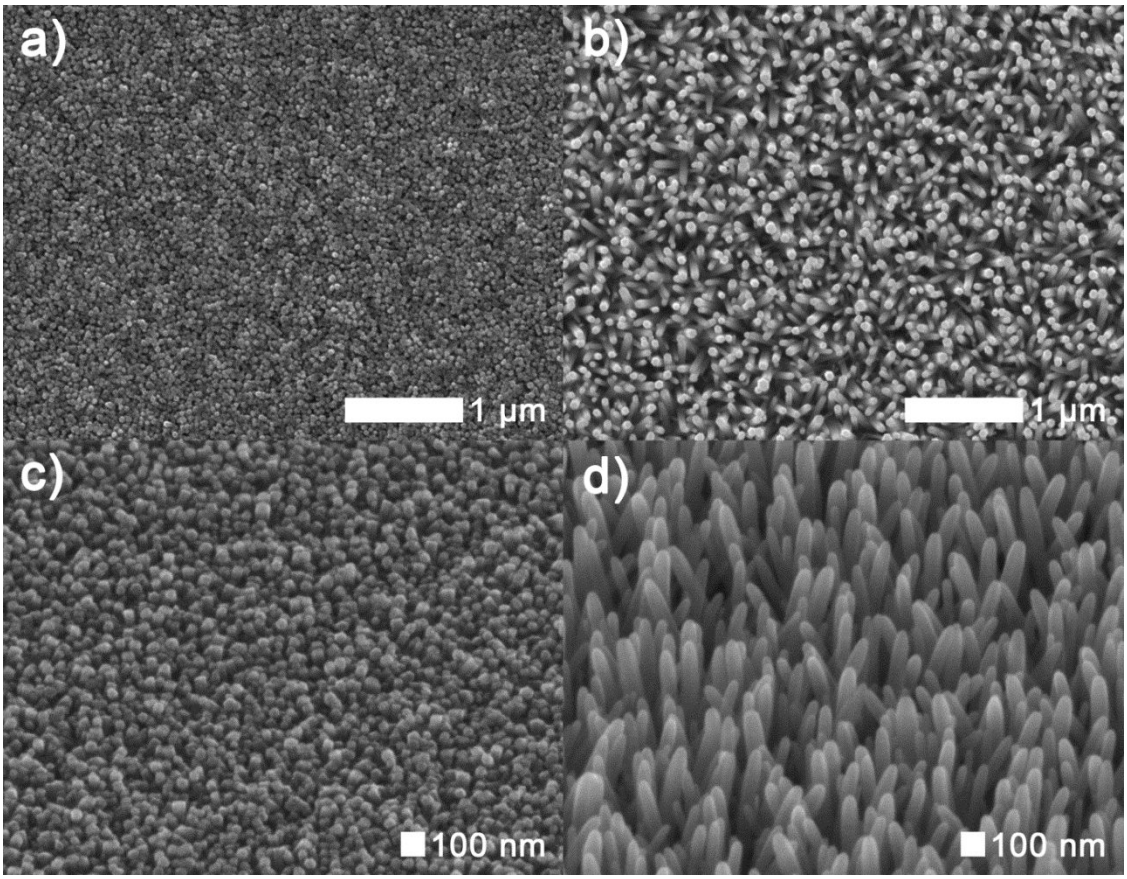

Figure 2. Top view and tilt view SEM images of ZnO nanorods with different growth time: a) 40 min top view; b) 3 h top view; c) 40 min tilt view; d) 3 h tilt view.

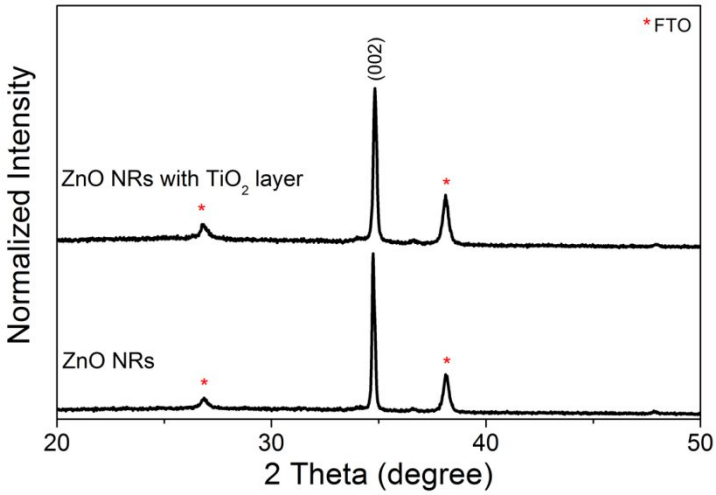

Figure 3. XRD pattern of as grown ZnO nanorods and ZnO nanorods with 5 nm TiO_2 layer by ALD.

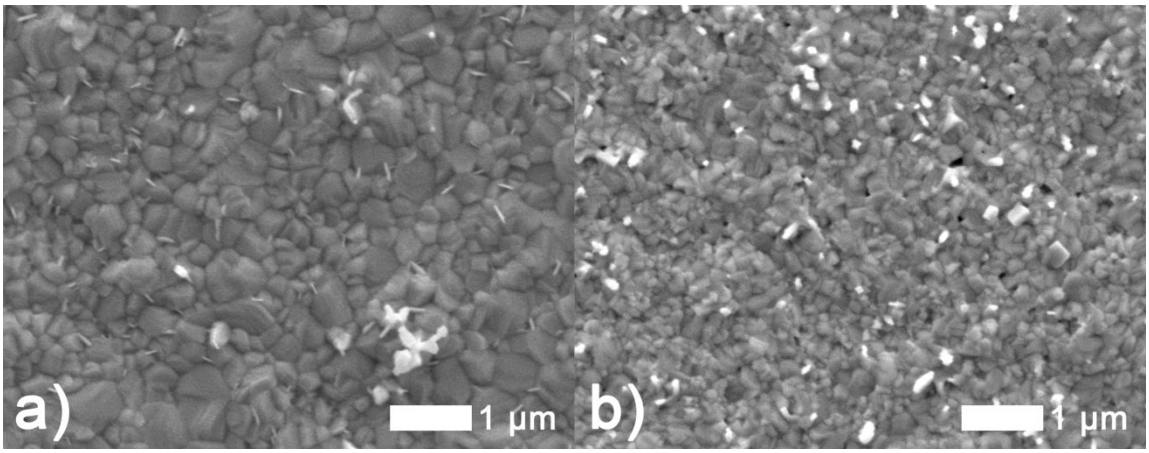

Figure 4. SEM images of perovskite films synthesized on a) as prepared ZnO thin film and b) ZnO thin film with 5 nm TiO_2 layer.

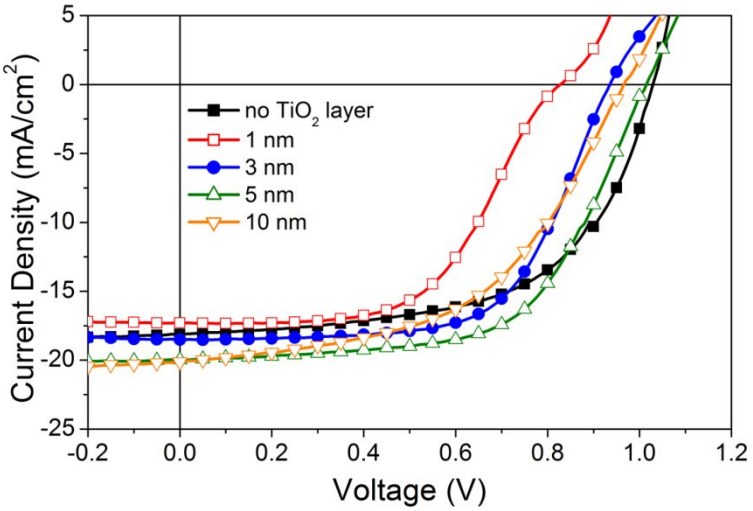

Figure 5. I-V characterization of devices based on ZnO thin films with different TiO_2 layer thicknesses.

Table 1. Solar cell performance parameters of ZnO thin film based devices with different TiO_2 layer thicknesses.

	J_{sc} (mA/cm^2)	V_{oc} (V)	FF	PCE (%)
No TiO_2	18.1	1.03	0.59	10.9
1 nm TiO_2 layer	17.3	0.83	0.56	8.0
3 nm TiO_2 layer	18.5	0.94	0.63	10.9
5 nm TiO_2 layer	20.0	1.02	0.61	12.3
10 nm TiO_2 layer	20.1	0.97	0.51	10.0

To investigate the influence of TiO_2 layer thickness on the performance of the perovskite solar cells, devices were prepared on as prepared ZnO thin films as well as ZnO thin films with 1 nm, 3 nm, 5 nm, and 10 nm of TiO_2 layer respectively. The J-V curves of the best performing devices based on ZnO ETLs are shown in Figure 5. It can be observed that with the addition of TiO_2 passivation layer the open circuit voltage decreased regardless of the TiO_2 layer thickness. 1 nm TiO_2 layer results in worse photovoltaic performance compared to the control device. Nevertheless, with the increase of the layer thickness, ZnO/TiO_2 based devices exhibited improved short circuit current and fill factor. The optimized device performance is obtained with 5 nm TiO_2 layer, with the best performing cell exhibiting short circuit current density of 20.0 mA/cm^2, open circuit voltage of 1.02 V, and fill factor of 0.61, resulting in power conversion efficiency (PCE) of 12.3% under reverse scan. For the device with 10 nm TiO_2 layer, decreases in open circuit voltage and fill factor are observed resulting in a decreased power conversion efficiency. The obtained device performance indicates that in general, TiO_2 layer on ZnO thin film can enhance charge collection at perovskite/metal oxide interface, which leads to a enhanced short circuit current. A optimized thickness of 5 nm can result in enhanced overall device performance.

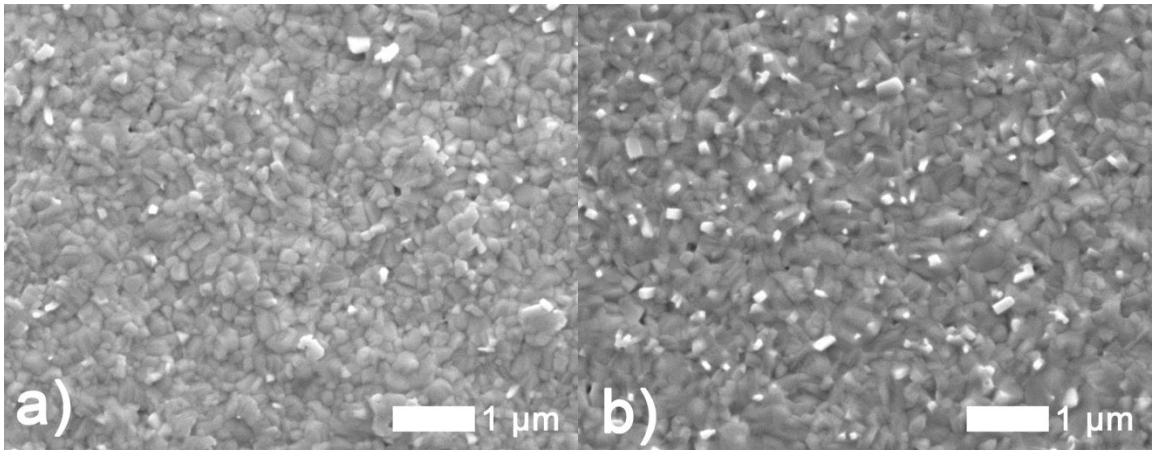

Figure 6. SEM images of perovskite films synthesized on a) short ZnO nanorods with 5 nm TiO_2 layer, and b) long ZnO nanorods with 5 nm TiO_2 layer.

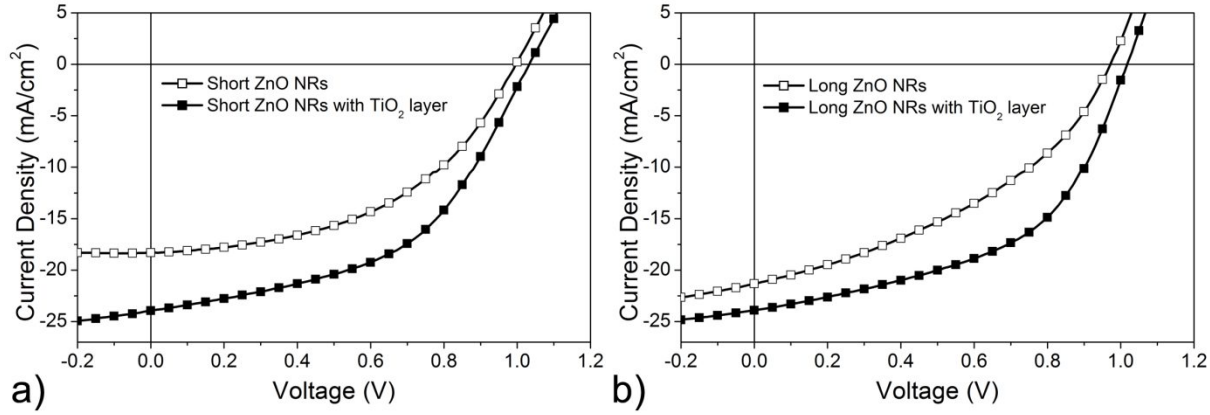

Figure 7. I-V characterization of ZnO NRs based devices with and without TiO_2 layer: a) ZnO NRs grown at 40 min; b) ZnO NRs grown at 3 h.

Table 2. Solar cell performance parameters of ZnO nanorod based devices.

	J_{sc} (mA/cm^2)	V_{oc} (V)	FF	PCE (%)
Short NRs	18.3	1.00	0.48	8.8
Short NRs with TiO_2	23.9	1.04	0.49	12.2
Long NRs	21.3	0.98	0.39	8.1
Long NRs with TiO_2	21.4	0.94	0.51	10.1

Based on the obtained results from devices with planar ZnO/TiO_2 ETLs, we have further investigated the influence of TiO_2 passivation layers on ZnO nanorods based devices. The optimized thickness of 5 nm is used for both short ZnO nanorods grown at 40 min and long nanorods grown at 3 h. SEM images of the perovskite films synthesized on different ZnO nanorods with TiO_2 layers are shown in Figure 6. The comparison of device performance with and without TiO_2 layer is shown Figure 7. It is clearly observed that 5 nm of TiO_2 layer can significantly enhance the device performance, and the enhancement is more significant compared to the devices based on ZnO thin films. In particular, the fill factor is enhanced in both devices with different rod growth time. Comparison of I-V curves of best performing devices with short nanorods and long nanorods with TiO_2 layers is shown in Figure 8. Nanorod morphologies (densities, apect ratios) are reported to have direct influence on PSC device performances.[7] Here it can be indicated that though longer ZnO

nanorods exhibit higher aspect ratio, the device performance is inferior to the devices with short nanorods. This is mainly attributed to the decrease of short circuit current and open circuit voltage with long nanorods. For the short nanorods with the growth time of 40 min, on the one hand the increased aspect ratio compared to ZnO thin films allows better charge collection at the interface, resulting in increased short circuit current from 20.0 mA/cm^2 to 23.9 mA/cm^2; on the other hand the morphology is more compact compared to longer nanorods, which may be beneficial to the perovskite/metal oxide interlayer, resulting in slightly increased open circuit voltage. Further optimization is required to improve the fill factor of the devices based on ZnO nanorods to improve their photovoltaic performance. Nevertheless, ZnO nanorods have demonstrated considerable potential as an electron transport scaffold layer for perovskite solar cells if with proper surface engineering.

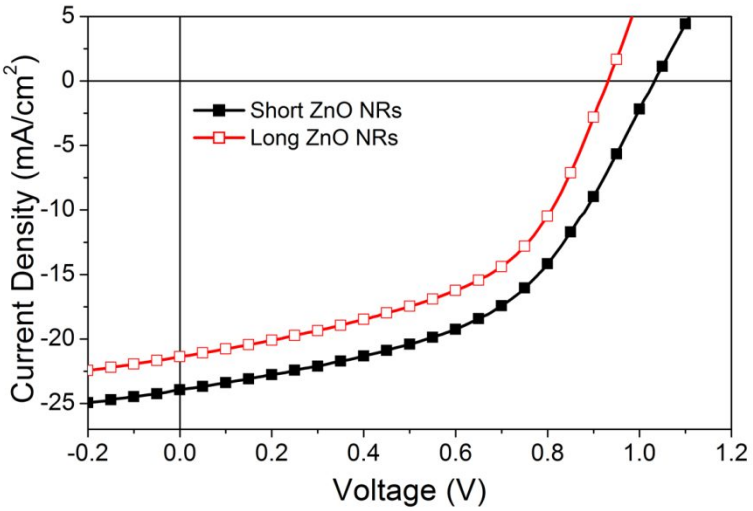

Figure 8. I-V characterization of the best performing devices based on short ZnO nanorods with TiO_2 layer and long ZnO nanorods with 5 nm TiO_2 layer.

4. CONCLUSIONS

In this work, the effect of TiO_2 passivation layer on ZnO nanostructures is investigated. An ultrathin TiO_2 layer with precisely controllable thickness is deposited on ZnO thin films and ZnO nanorods with different growth time. It is indicated that with an optimized thickness of 5 nm, such TiO_2 layer can effectively enhance the device performance. ZnO nanorods exhibit considerable potential as electron transport scaffolds for perovskite solar cells, while the nanorod morphology can directly affect the device performance.

Acknowledgement

Financial support from the ECF project 35/2015, as well as Strategic Research Theme, University Development Fund, and Seed Funding for Basic Research of the University of Hong Kong is acknowledged.

REFERENCES

[1] Jung, H. S., Park, N.-G., "Perovskite solar cells: From materials to devices," *Small* 11, 10-25 (2015).

[2] Kim, H.-S. Lee, C.-R., Im, J.-H., Lee, K.-B., Moehl, T., Marchioro, A., Moon, S.-J., Humphry-Baker, R., Yum, J.-H., Moser, J. E., Grätzel, M., and Park, N.-G., "Lead iodide perovskite sensitized all-solid-state submicron thin film mesoscopic solar cell with efficiency exceeding 9%," *Sci. Rep.* 2, 591 (2012).
[3] Lee, M. M., Teuscher, J., Miyasaka, T., Murakami, T. N., and Snaith, H. J., "Efficient hybrid solar cells based on meso-superstructured organometal halide perovskites," *Science* 338, 643-674 (2012).
[4] Yang, W. S., Park, B.-W., Jung, E. H., Jeon, N. J., Kim, Y. C., Lee, D. U., Shin, S. S., Seo, J., Kim, E. K., Noh, J. H., and Seok, S. I., "Iodide management in formamidinium-lead-halide–based perovskite layers for efficient solar cells," *Science* 356, 1376-1379 (2017).
[5] Kumar, M. H., Yantara, N., Dharani, S., Grätzel, M., Mhaisalkar, S., Boix, P. P., and Mathews, N., "Flexible, low-temperature, solution processed ZnO-based perovskite solid state solar cells," *Chem. Commun.* 49, 11089-11091 (2013).
[6] Son, D.-Y., Im, J.-H., Kim, H.-S., and Park, N.-G., "11% efficient perovskite solar cell based on ZnO nanorods: An effective charge collection system," *J. Phys. Chem. C* 118, 16567-16573 (2014).
[7] Xu, Y., Liu, T., Li, Z., Feng, B., Li, S., Duan, J., Ye, C., Zhang, J., and Wang, H., "Preparation and photovoltaic properties of perovskite solar cell based on ZnO nanorod arrays," *Appl. Surf. Sci.* 388, 89-96 (2016).
[8] Guo, Y., Li, X., Kang, L. L., He, X., Ren, Z. Q., Wu, J. D., and Qi, J. Y., "Improvement of stability of ZnO/ $CH_3NH_3PbI_3$ bilayer by aging step for preparing high-performance perovskite solar cells under ambient conditions," RSC Adv. 6, 62522-62528 (2016).
[9] Mahmood, K., Swain, B. S., and Amassian, A., "16.1% efficient hysteresis-free mesostructured perovskite solar cell based on synergistically improved ZnO nanorod arrays," *Adv. Energy Mater.* 5, 1500568 (2015).
[10] Si, H. N., Liao, Q. L., Zhang, Z., Li, Y., Yang, X. H., Zhang, G. J., Kang, Z., Zhang, Y., "An innovative design of perovskite solar cells with Al_2O_3 inserting at ZnO/perovskite interface for improving the performance and stability," *Nano Energy* 22, 223–231 (2016).
[11] Dong, J., Zhao, Y. H., Shi, J. Q., Wei, H. Y., Xiao, J. Y., Xu, X., Luo, J. H., Xu, J., Li, D. M., Luo, Y. H., and Meng, Q. B., "Impressive enhancement in the cell performance of ZnO nanorod-based perovskite solar cells with Al-doped ZnO interfacial modification," *Chem. Commun.* 50, 13381-13384 (2014).
[12] Wang, B. X., Liu, T. F., Zhou, Y. B., Chen, X., Yuan, X. B., Yang, Y. Y., Liu, W. P., Wang, J. M., Han, H. W., and Tang, Y. W., "Hole-conductor-free perovskite solar cells with carbon counter electrodes based on ZnO nanorod arrays," *Phys. Chem. Chem. Phys.*18, 27078-27082 (2016).
[13] Dong, Q., Liu, F. Z., Wong, M. K., Tam, H. W., Djurišić, A. B., Ng, A., Surya, C., Chan, W. K., and Ng, A. M. C., "Encapsulation of perovskite solar cells for high humidity conditions, " *ChemSusChem* 9, 2597-2603 (2016).
[14] Dkhissi, Y., Meyer, S., Chen, D., Weerasinghe, H. C., Spiccia, L., Cheng, Y.-B., and Caruso, R. A., "Stability comparison of perovskite solar cells based on zinc oxide and titania on polymer substrates," ChemSusChem 9, 687-695 (2016).
[15] Yang, J., Siempelkamp, B. D., Mosconi, E., De Angelis, F., and Kelly, T. L., "Origin of the thermal instability in $CH_3NH_3PbI_3$ thin films deposited on ZnO," *Chem. Mater.* 27 4229-4236 (2015).
[16] Liu, F. Z., Dong, Q., Wong, M. K., Djurišić, A. B., Ng, A., Ren, Z., Shen, Q., Surya, C., Chan, W. K., Wang, J., and Ng, A. M. C., "Is Excess PbI_2 Beneficial for Perovskite Solar Cell Performance?" *Adv. Energy Mater.*6, 1502206 (2016).